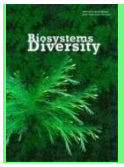

Biosystems Diversity

ISSN 2519-8513 (Print)
ISSN 2520-2529 (Online)
Biosyst. Divers.

Anatomical diagnostic indicators of adaptation to ecological conditions in the vegetative and generative organs of *Peganum harmala* (Nitrariaceae)

A. Sardarova

Azerbaijan State Agricultural University, Ganja, Azerbaijan

Article info

Received 16.07.2025
Received in revised form 24.08.2025
Accepted 27.09.2025

Azerbaijan State Agricultural University, Ozan st., Ganja, AZ2007, Azerbaijan.
Tel.: +994-604-44-42.
E-mail: aygun.sardarova4442@gmail.com

Sardarova, A. (2025). Anatomical diagnostic indicators of adaptation to ecological conditions in the vegetative and generative organs of Peganum harmala (Nitrariaceae). Biosystems Diversity, 33(4), e2555. doi:10.15421/012555

One of the priority directions in modern botany is the experimental investigation of the ecological anatomy of plants. Rapidly increasing anthropogenic pollution is among the main ecological issues threatening ecosystem stability and plant diversity on a global scale. In this context, studying the adaptive mechanisms of species resistant to ecological pressures, including plants with bioindicator potential such as *Peganum harmala*, holds particular significance. Such studies provide not only an assessment of regional conditions but also a scientific basis for global phytobioindication, biodiversity conservation, and ecological restoration strategies. Investigating the structural adaptations of flora elements in ecologically pristine and phytocontaminated environments is crucial for evaluating ecosystem health. The present study is distinguished by a comprehensive approach analyzing structural adaptations of plants under contemporary ecological risks, thereby integrating regional observations into the study of global environmental challenges. Plant samples naturally occurring in the study areas were collected, fixed, and subjected to anatomical sectioning. Transverse sections obtained using a microtome were treated with histochemical reagents and processed into permanent preparations. Statistical analysis of micrometric parameters recorded during microscopic examination revealed significant differences among the samples. Notably, in plants collected from the Aghdam Industrial Park, massive accumulation of yellow-pigmented intracellular inclusions was microscopically confirmed in the palisade parenchyma of leaves, the prosenchymatous tissue of the petiole, the palisade cell layer of the sepal, and the chlorenchyma of the stem and pedicel. Parenchymatic inclusions were also observed. Idioblasts were recorded in both leaves and sepals of these samples. Statistical measurements indicated that in the Aghdam specimens, the thickness of chloroplast-containing parenchyma layers in leaves, petioles, and sepals was greater, whereas in the Zangilan specimens, the epidermal cell size and the thickness of their outer periclinal walls were higher across all above-ground vegetative organs. In seeds from Zangilan, the aleurone layer was better developed, while in the Aghdam seeds, a thicker endotesta and accumulation of non-specific intracellular inclusions were observed, demonstrating that structural variability occurs under differing environmental conditions. Root samples from Aghdam showed more compact tissue organization, particularly a thicker periderm and stronger sclerenchyma development. These findings highlight the plant's high adaptive capacity and visually confirm the localization of non-specific inclusions at the anatomical level. The accumulation of such inclusions in medicinal plants exposed to phytocontamination may pose risks to their medicinal use. Given that *P. harmala* is widely employed as a medicinal plant, investigating non-specific deposits within its internal structures under contaminated conditions provides essential scientific evidence for assessing the ecological safety of medicinal plants and for selecting appropriate cultivation environments.

Keywords: isobilateral leaf; phytocontamination; prismatic styloid and raphide type crystals; intracellular inclusions; idioblast; anthropogenic dynamics of the ecosystem.

Introduction

In contemporary botanical research, the analysis of anatomical structures of plant organs extends beyond the study of morphological and anatomical traits of flora elements. It also plays a crucial role in identifying cellular-level imprints of various ecological factors, including anthropogenic impacts, pollution, and stress conditions. Microscopic analyses of plant tissues often reveal diverse intracellular and intercellular deposits that are visually distinguishable but whose precise chemical composition has not yet been fully elucidated. Such deposits are commonly characterized as endogenous or exogenous intracellular and intercellular inclusions, and their formation may be considered as potential biomarkers of plant responses to environmental conditions. The presence of these structures, on the one hand, provides insights into plant adaptation mechanisms, and on the other hand, opens new opportunities for monitoring ecotoxicological processes. These nonspecific local accumulations, documented at the anatomical level, are likely associated with metabolic and physiological alterations in plants. Therefore, future research into their origin at phytochemical, biochemical, isotopic, and molecular levels is of paramount importance. Within the framework of modern ecological anatomy, the study of such structures is relevant not only for fundamental botany but also for ecological risk assessment, bioremediation, and environmental health monitoring. *Peganum harmala* L., a perennial herbaceous plant of the family Nitrariaceae Lindl. (Benlarbi & Chaachouay, 2025), occurs across various geographical regions and has a wide natural distribution range in the arid and saline territories of the Republic of Azerbaijan (Qurbanov, 2024). *Peganum harmala* is regarded as a pseudometallophyte since it can grow both in ecologically clean habitats and in ecotopes contaminated with heavy metals (El Hasnaoui et al., 2023). Studies of plant species inhabiting areas with heavy metals and other pollutants demonstrate that species with a high adaptive capacity exhibit phytocontamination-related responses at physiological and anatomical levels with pronounced intensity (Čiamporová et al., 2021; Collin et al., 2022; Han et al., 2022; Singh et al., 2022; Muszyńska et al., 2023), thereby ensuring biodiversity persistence under such stressful conditions. In medicinally important plant species, the study of such adaptation-related processes and the consequent physiological, biochemical, and morphological changes is particularly significant (Ahmad et al., 2021; Krzesłowska et al., 2021; Ait Elallem et al., 2022). Previous research has shown that stress conditions may alter the efficiency of metabolite synthesis.

As a medicinal plant, *P. harmala* contains a rich array of secondary metabolites, including harman, harmaline, harmine, quinazoline, alkaloids, and others (Doskaliyev et al., 2021; Li, 2024; Say, 2024). Pharmacologically, the species is used in the treatment of cardiovascular, nervous, respiratory, and endocrine disorders, and it also exhibits antimicrobial activity (Shahrajabian et al., 2021; Akhtar et al., 2022; Zhu et al., 2022; Ibadullayeva, 2024). Several studies investigating *P. harmala* in contaminated environments have focused on the

impact of pollutants on assimilation processes, while also demonstrating that the species possesses metabolic mechanisms that confer resistance to oxidative stress induced by heavy metals (Mahdavian, 2022; Basahi, 2023).

The primary objective of our study was to perform a comparative ecological-anatomical analysis of *P. harmala* specimens collected from two distinct areas of the Karabakh region of Azerbaijan: an industrially polluted site and a relatively undisturbed natural site. This comparison aimed to identify structural variations and to evaluate the intensity of phytocontamination. A number of studies conducted by foreign researchers have revealed physiological adaptation processes and response mechanisms in other plant species under stress conditions induced by various factors (Karim et al., 2024; Ullah et al., 2024; Yirmibeş et al., 2024; Gao et al., 2025; Seven & Akıncı, 2025). In line with the author's earlier works (Sardarova, 2024, 2025a, 2025b; Sardarova & Ibadullayeva, 2025), the present study provides an alternative perspective by approaching the problem at the anatomical level. This enables the exploration of the adaptive potential of the species, the occurrence of specific and nonspecific intracellular and intercellular localizations, and the structural modifications arising in the plant under varying environmental conditions.

In a globalized world, the intensification of anthropogenic pressures significantly disrupts the structural and functional stability of ecosystems. Factors such as urbanization, industrial emissions, and the pollution of soil and water bodies lead to the emergence of unusual morpho-anatomical alterations in plants. Among the most important indicators of such changes are intracellular and intercellular deposits of unknown origin. The occurrence of these structures – various intracellular and intercellular localizations whose precise origin remains unclear – plays a pivotal role in plant physiological and metabolic responses. Their detection is only possible through high-resolution anatomical studies, which today constitute one of the most relevant and strategically important directions in the study of plant adaptation mechanisms.

Considering the medicinal significance of *P. harmala*, the plant investigated in this study, it should be emphasized that the analysis of such inclusions in phytotherapeutically valuable species holds particular relevance. Deposits formed through bioaccumulation processes may serve as critical indicators of both plant adaptation to ecological stress factors and the synthesis and storage of secondary metabolites. At the same time, these structures can function as biomarkers for monitoring heavy metals, toxic elements, and other contaminants under ecotoxicological conditions. Thus, the anatomical investigation of inclusions of unknown origin provides new opportunities not only for theoretical botany but also for applied disciplines such as ecological anatomy, phytotoxicology, biomonitoring, and pharmacognosy. In an era of increasing anthropogenic dynamics within ecosystems, such an approach is essential for the conservation and sustainable use of medicinal plants, as well as for assessing their metabolic potential under stress conditions.

The accumulation of inclusions of unidentified origin in plant organs can initially be visualized and assessed through anatomical methods, after which they may be subjected to complementary research. Anatomical studies are regarded as the first key stage, laying the foundation for further scientific contributions. This approach is recognized as one of the most advanced and relevant scientific directions for elucidating plant responses to ecological stressors. The study of such inclusions in flora elements – especially in medicinally important species – facilitates the interpretation of their adaptation mechanisms while also contributing to the identification of bioaccumulation processes, phytotoxins, or potential biomarkers. Therefore, anatomical investigations of deposits establish a fundamental scientific basis for assessing ecological plasticity, tolerance strategies, and metabolic restructuring potential in plants under stress conditions. Through ecological-anatomical methods, the visualization of critical structural features of ecosystems under ecological pressure represents a modern and strategically significant research direction in plant ecophysiology and stress biology. In conclusion, in the current era of heightened anthropogenic dynamics, the anatomical study of inclusions of unknown origin in medicinal plants is of great importance not only for fundamental botany but also for applied areas such as sustainable ecosystem management, medicinal plant conservation, and biodiversity maintenance. Furthermore, this approach, by linking with global scientific priorities such as climate change, biocontamination, and bioremediation processes, offers innovative opportunities for managing ecological risks.

The investigation of *P. harmala*'s ability to adapt to diverse ecological conditions provides insights into its autoecological traits and allows an evaluation of its structural adaptations to stress factors. Although the species demonstrates normal development in terms of morphological indicators, anatomical studies confirm that it has been exposed to contamination. In specimens of *P. harmala* collected from polluted environments, inclusions were observed as indicators of biochemical and physiological changes resulting from phytocontamination. The study documented the formation of nonspecific intracellular deposits, further confirming that the ecological-anatomical study of plants represents one of the most pressing issues in modern experimental botany. The findings emphasize that anatomical analyses serve as more sensitive biomarkers than morphological observations, enabling precise assessment of plant ecological status. Consequently, the results demonstrate the potential risks associated with the medicinal and nutritional use of plants collected from contaminated habitats, highlighting the significance of anatomical research in ecological safety and phytosanitary evaluation.

Finally, the structural comparison of ecotypes of this species provides valuable markers for predicting the responses of modern flora elements to similar ecological conditions, thereby contributing to the broader understanding of plant adaptation under anthropogenic stress.

Materials and methods

Collection and laboratory processing of material. Comparative ecological and anatomical analyses of the medicinally valuable species *P. harmala* were conducted using specimens collected from two sites in the Karabakh region of Azerbaijan: the industrially contaminated zone near Aghdam Industrial Park (Fig. 1a, 1c) and the ecologically clean area near Bartaz village, Zangilan district (Fig. 1b, 1d). After collection, the plant materials were stabilized using appropriate fixation methods (Chamberlain, 2020; Criswell et al., 2025) and subsequently processed under laboratory conditions.

During laboratory preparation, paraffin (BW Blended Waxes, Inc., USA) was used as a supporting medium during both tissue infiltration and sectioning. Sections were prepared using a modern hand microtome (RADICAL, RMT-5, India), and the section thickness was precisely calibrated and controlled via a micrometric adjustment screw (Fig. 2). Tissue slices with a thickness of approximately 8 μm were obtained through micrometric regulation.

Following sectioning, histochemical methods were applied, and differential staining was performed using specific reagents. A set of selective stains, including Safranin O, Fast Green, Sudan III, Toluidine Blue, Phloroglucinol-HCl, and Methylene Blue (KimyaLab, Turkey), were utilized (Fig. 3). The staining process was conducted stepwise using a decolorization technique to ensure the selective visualization of tissue components (Peterson et al., 2008; Bozdağ et al., 2016; Da Silva et al., 2020; Engin et al., 2024). The sequential application of various histological stains facilitated a more precise identification of ecological-anatomical structural features in both *P. harmala* ecotypes. Additionally, chemical reagents such as xylene, carboxylol, ethylene, formalin, and chlorinated lime (Mir Nauki, Russia) were employed to support tissue dehydration and enhance the clarity of anatomical structures, thereby enabling more effective microscopic observations. To prepare permanent microscope slides from the stained sections, Canada balsam (Innovating Science, USA) was used as a mounting medium (Fig. 3b). A drop of balsam was applied to the section placed on a glass slide, followed by the placement of a coverslip. The prepared slides were then placed in a special incubator device set at a constant temperature of 20–25 °C to allow the Canada balsam to dry completely. Once the mounting medium had fully cured, the permanent transverse sections were subjected to detailed microscopic analysis.

Fig. 1. The general view of *Peganum harmala* (L.) (*a*, *b*) and the areas where plant samples were collected: *c* – Aghdam Industrial Park area (contaminated area), *d* – Zangilan District, Bartaz Village (near the Araz River) (clean area)

Fig. 2. Preparation of permanent slides (cutting and histology staining stage)

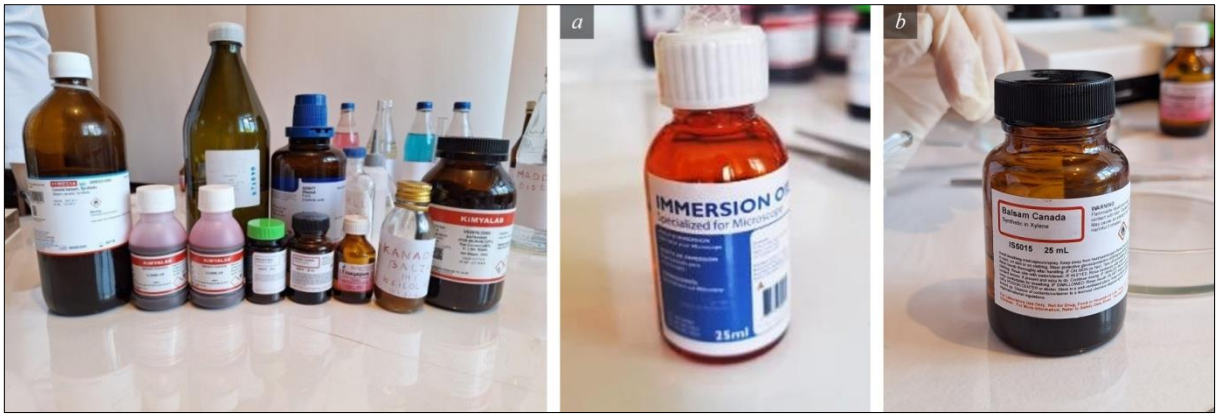

Fig. 3. Some reagents used in the research work: *a* – immersion oil; *b* – Canada balsam

Microscopic analysis. Microscopic investigations were conducted using advanced digital and multifunctional microscopes available at the Department of Biology, Azerbaijan State Agricultural University. Primarily, a Carl Zeiss Axio Imager A2 (ZEISS, Germany) microscope was employed (Fig. 4), which is equipped with a high-performance LED illumination system and specialized objectives designed to minimize optical aberration. This model offers exceptional optical performance, and Zeiss's AxioCam digital camera system was integrated into the microscope interface, ensuring advanced imaging capabilities. Utilizing the full potential of the Axio Imager A2 system, detailed structural analysis of *P. harmala* generative and vegetative organ preparations was performed. This included micrometric measurements, live video monitoring, and high-resolution digital microphotography.

In addition, the NLCD-307B LCD Digital Microscope (Wincom Company Ltd., China) was used during the course of the study (Fig. 5a, 5b). This microscope features an integrated LCD display, enabling real-time visual observation of the specimens directly on the

screen. Through its advanced digital imaging capabilities, high-precision ecological-anatomical assessments of *P. harmala* were successfully conducted. For accurate anatomical identification, the full range of objective magnifications (4×, 10×, 40×, 60×, and 100×) was utilized. Observations at 100× magnification were enhanced using immersion oil (RMY, USA), which significantly improved optical resolution and contrast of microscopic images (Fig. 3a). The NLCD-307B digital microscope was particularly useful during the early stages of sectioning, for monitoring the quality of tissue cuts and the effectiveness of histological staining before preparation of permanent slides. Final analyses, acquisition of photomicrographs, and statistical measurements were performed using the Carl Zeiss Axio Imager A2 system.

For macroscopic examination of plant specimens, stereomicroscopes were also used, specifically the Zeiss Stemi508 (ZEISS, Germany) and the Stereo YK-SM067B2 (Wincom Company Ltd., China) (Fig. 5c, 5d).

To ensure the precision of micrometric data obtained via automated measurements during microscopic analysis, eyepiece and stage micrometers (Muhva, China) were employed (Fig. 6a, 6b). First, the eyepiece micrometer was calibrated using the stage micrometer, after which specimen dimensions were calculated based on the scale divisions. Additionally, a digital macrometer (Jiavarry, China) was used to record macroscopic dimensions of plant organs prior to sectioning (Fig. 6c). All measurement data were properly annotated and overlaid on the corresponding photomicrographs (Jambor et al., 2021).

Fig. 4. Working with the Carl Zeiss Axio imager A2 optical microscope model

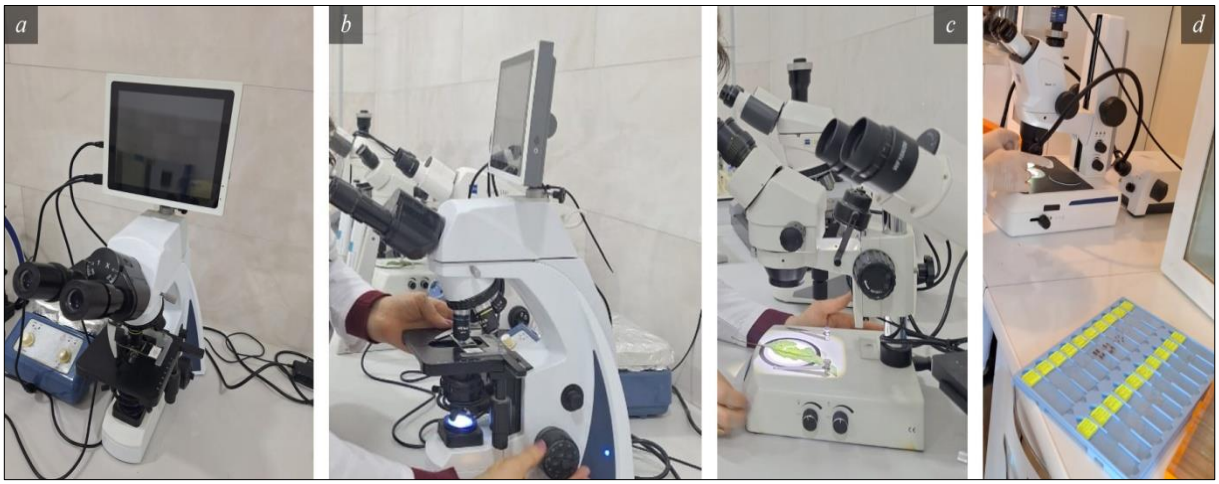

Fig. 5. Optical and stereoscopic microscopes used: *a*, *b* – LCD Dijital Microskop NLCD-307B, *c* – steoroscope Zeiss Stemi508, *d* – Stereo YK-SM067B2

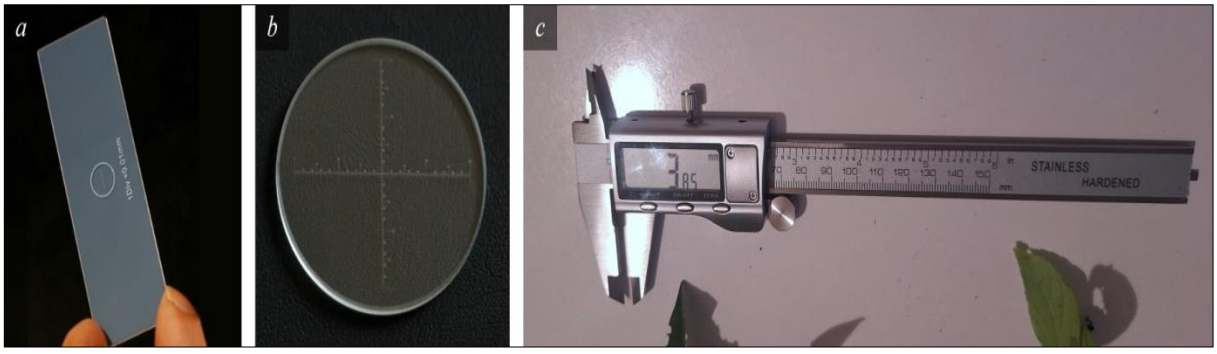

Fig. 6. Instruments used in the measurement process: *a* – stage micrometer, *b* – eyepiece micrometer, *c* – digital micrometer

Fig. 7. Preparation of herbarium

Herbarium preparation. Herbarium specimens prepared from the medicinally valuable species *P. harmala* serve not only as systematic resources for in-depth ecological and anatomical investigations, but also as key reference materials for evaluating the species' pharmacognostic and phytotherapeutic potential (Fig. 7). Herbarium samples were prepared from both *P. harmala* populations under investigation – those collected from ecologically distinct regions – and subsequently deposited into the herbarium collection of the Department of Biology named after Academician Valida Tutayuq at Azerbaijan State Agricultural University. These specimens are preserved as part of a systematically organized botanical collection and are available for scientific research, educational purposes, and reference use.

Statistical methods. Quantitative data obtained from the generative and vegetative organs of both sites were expressed as mean ± standard deviation (SD). The assumption of normal distribution was tested using the Shapiro–Wilk test, while homogeneity of variances was assessed by Levene's test. Since both assumptions were met, ANOVA was performed using Fisher's criterion. Statistical analyses were conducted with the Jamovi software (version 2.6.26; University of Sydney, Australia).

Results

Seed. Transverse section analysis revealed that the seed of *P. harmala* is externally surrounded by a thick testa. The largest cells of the testa are located in its outer exotesta layer. These cells function in mechanical protection and prevention of water loss. Possessing thickened walls, they were identified as columnar osteosclereid cells. Their basal ends are markedly thickened, thereby enhancing the mechanical strength of the seed. In samples from both studied sites, the exotesta was externally covered by a thick cuticular layer.

The second prominent layer of the testa is the internal endotesta. This layer performs functions of inner protection, water absorption, and maintenance of seed viability. Micrometric measurements confirmed statistically significant differences in the height of endotesta cells between the studied sites (Table 1). On average, endotesta cells were taller in seeds collected from the industrially polluted environment of the Aghdam Industrial Park. Moreover, microscopic observations revealed the presence of intracellular inclusions within these cells in the same polluted-area samples.

Table 1

Descriptive statistics (x ± SD, n = 15) and results of ANOVA test
for measurements obtained from seed samples of *Peganum harmala* (L.) collected from the study areas

Indicators	Mean ± SD, µm		ANOVA (Fisher's)			
	Aghdam (Aghdam Industrial Park area)	Zangilan (Bartaz village area)	F	df1	df2	p
Height of exotesta cells	165.63 ± 50.39	193.41 ± 53.79	0.912	1	28	3.6×10^{-1}
Thickness of the cuticle layer	11.20 ± 2.58	14.65 ± 2.16	5.850	1	28	3.8×10^{-2} *
Diameter of mesotest acells	27.48 ± 8.53	20.78 ± 3.22	2.760	1	28	1.2×10^{-1}
Height of endotesta cells	136.87 ± 30.02	97.58 ± 9.27	23.466	1	28	4.2×10^{-5} ***
Diameter of endosperm cells	38.56 ± 5.20	31.24 ± 5.62	6.776	1	28	2.1×10^{-2} *

Note: SD – standard deviation; normality was confirmed for all measurements based on the Shapiro-Wilk test (P > 0.05); homogeneity of variances was assessed using Levene's test; measurements met the homogeneity assumption (P > 0.05); significance level of the difference: * – P < 0.05; ** – P < 0.01; *** P < 0.001.

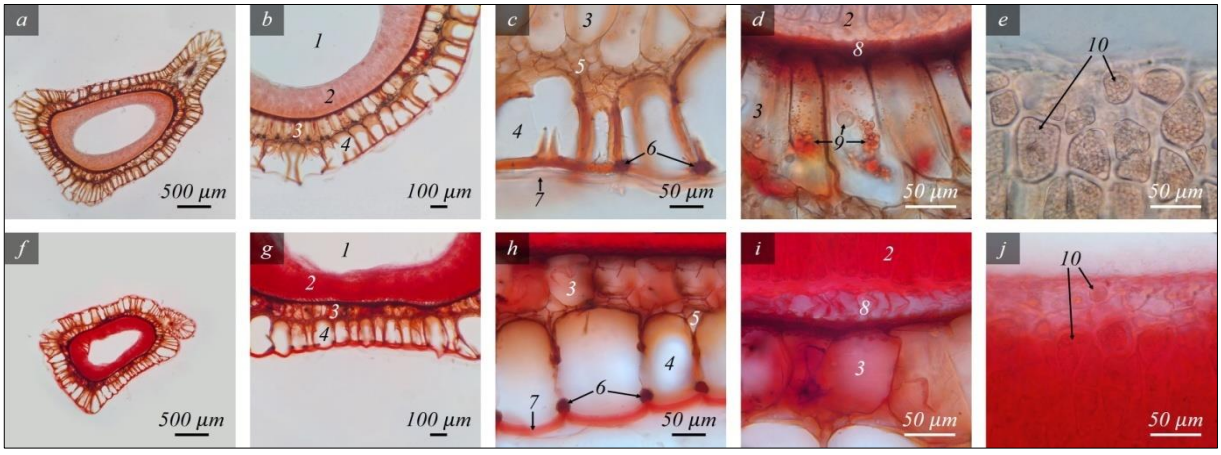

Fig. 8. Transverse sections of *Peganum harmala* (L.) seed samples from Aghdam (top row) and Zangilan (bottom row) (section thickness – 8 µm): *a, f* – general view of the section, *b, g* – a part of the section, *c, h* – outer side of the testa, *d, i* – boundary between testa and endosperm, *e, j* – endosperm layer; *1* – embryo cavity, *2* – endosperm, *3* – endotest, *4* – exotest, *5* – mesotest, *6* –- thickened basal ends of osteosclereid cells, *7* – cuticle, *8* – aleurone layer, *9* – intracellular inclusion, *10* – ergastoplasm granules accumulated in endosperm cells

The middle layer of the testa is represented by the mesotesta. Its cells are relatively small, morphologically variable, and situated between the exotesta and endotesta, serving as an additional protective layer.

At the boundary of the testa and endosperm lies the aleurone layer (Fig. 8). This layer constitutes the outermost part of the endosperm and functions as a storage tissue that becomes physiologically active during germination. The aleurone layer is rich in proteins, lipids, and enzymes. During germination, these reserves are degraded, providing nutrients for the developing embryo. The proteins include enzymes (e.g., proteases and lipases) that catalyze the hydrolysis of storage compounds, thereby accelerating germination. In the arid and saline soils where *P. harmala* grows, the aleurone layer contributes to the long-term viability of seeds. Its thickness and high pigmentation enhance resistance against UV radiation and oxidative stress. Under stress conditions, this layer also plays a role in the accumulation of antioxidant compounds. Partial pigmentation of the aleurone layer provides additional protection against microbial and fungal infections, while simultaneously contributing to the mechanical durability of the seed.

From an ecological-anatomical perspective, seeds collected from ecologically clean sites exhibited a distinctly thick and well-differentiated aleurone layer. Protein bodies were more abundant and uniformly distributed, while pigmentation was at normal levels, thus ensuring protection against solar radiation and microorganisms. Nutrient reserves (proteins and lipids) were maintained at higher levels, resulting in greater germination energy. In contrast, seeds collected from contaminated habitats displayed a thinner, irregularly differentiated aleurone layer. Protein body content was reduced, and vacuolization was inconsistently observed. Microscopic analysis also showed weaker pigmentation. Consequently, diminished nutrient reserves were associated with reduced germination capacity and shortened seed viability. In *P. harmala*, the aleurone layer ensures optimal storage and protection under ecologically clean conditions; however, in contaminated sites, both the morphology and chemical composition of the layer are altered, with declines in protein and lipid content negatively affecting seed viability and adaptive potential.

Beneath the aleurone layer, the endosperm is composed of cells densely packed with ergastoplasmic granules. These granules represent spherical storage inclusions containing primarily starch, proteins, and lipids, thereby serving as the principal nutrient reserve for the embryo during its development. The endosperm layer is thick and surrounds the embryonic cavity. Overall, microscopic observations demonstrated that across all seed layers, pigmentation was particularly pronounced in the endosperm of samples collected from the Zangilan site.

Sepal. Transverse section analysis of the sepal in *P. harmala* revealed that specimens from the Aghdam site exhibit a more pronounced upward convexity compared to those from Zangilan. The vascular system of the sepal consists of a large central bundle located in the middle, accompanied by several smaller lateral bundles arranged sequentially on either side. Mechanical elements were not detected within these bundles. However, idioblasts were observed at the boundary of the central bundle only in samples from the Aghdam site. These idioblasts are assumed to function primarily in the storage of water, metabolites, and nutrient reserves, as suggested by their transparent vacuoles under microscopic observation (Fig. 9).

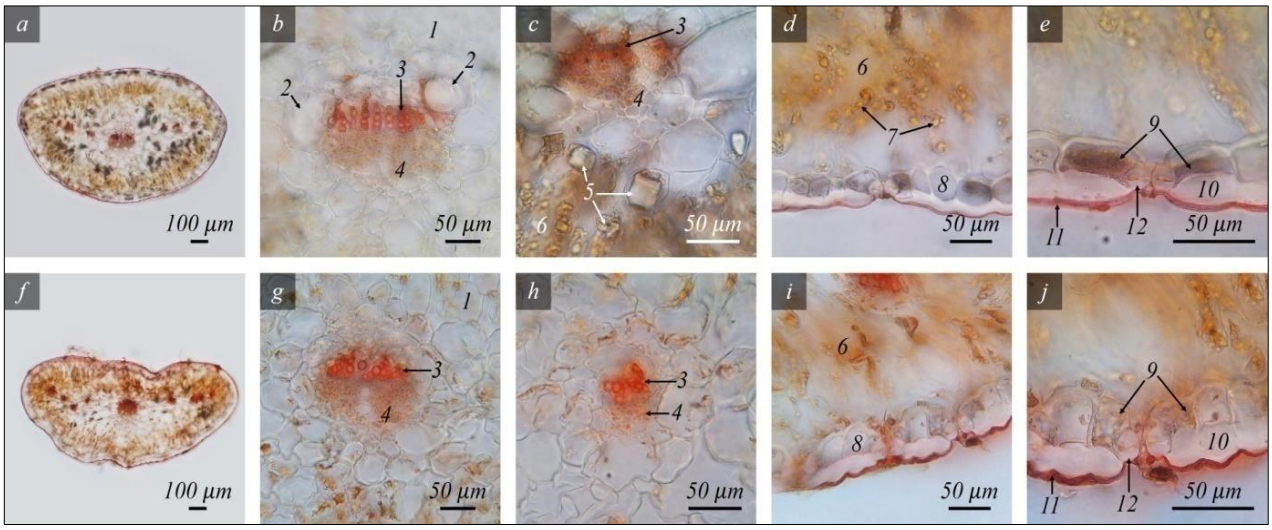

Fig. 9. Transverse sections of *Peganum harmala* (L.) sepal samples from Aghdam (top row) and Zangilan (bottom row) (section thickness – 8 µm): *a*, *f* – general view of the section, *b*, *g* – central vascular bundle, *c*, *h* – lateral vascular bundle, *d*, *i* – peripheral part of the sepal, *e*, *j* – structural features of the epidermis and stomatal apparatus; *1* – parenchyma area around the bundles, *2* – idioblast cells, *3* – xylem, *4* – phloem, *5* – prismatic and steloid-type crystals at the boundary with palisade-type parenchyma, *6* – palisade-type parenchyma, *7* – intracellular inclusions, *8* – epidermis, *9* – accumulation of ergastic and constitutive substances in the epidermis, *10* – thickened outer periclinal wall of the epidermis, *11* – cuticle layer, *12* – guard cells

Surrounding the vascular tissues is a parenchymatous zone composed of isodiametric cells of varying sizes. In samples from Aghdam, these cells contained prismatic crystals and other irregularly shaped inclusions. This parenchymatous zone is entirely enveloped by a tissue layer consisting of chloroplast-rich cells. Being a modified leaf organ, the sepal primarily functions as a protective structure for the flower, with limited photosynthetic capacity. Nevertheless, in perennial and drought-tolerant species, sepals may acquire enhanced photosynthetic activity due to a higher abundance of chloroplasts.

Anatomical analysis demonstrated that in the sepals of *P. harmala*, a fully differentiated palisade parenchyma, typical of classical leaf laminae, was not observed. Instead, an elongated, chloroplast-containing, densely arranged palisade-like cell layer was recorded. This indicates that sepals in *P. harmala* are not exclusively protective, but also partially contribute to photosynthetic activity. Importantly, this anatomical feature is reported here for the first time as an adaptive trait in *P. harmala* and may be regarded as a diagnostic indicator of the species' ecological resilience across different habitats.

In Aghdam samples, additional non-specific intracellular deposits were detected as yellow-orange droplets within palisade-like parenchyma cells. Furthermore, comparative analysis of sepals from both sites revealed that the concentration of ergastic and constitutive substances in the epidermal cells was higher in plants growing under contaminated conditions in the Aghdam Industrial Park. Epidermal cells were covered by a distinctly visible cuticle layer, which appeared darker in samples from Zangilan. Micrometric measurements and variation analysis further confirmed that the height of epidermal cells and the thickness of their periclinal walls were statistically greater in *P. harmala* specimens from the Zangilan site (Table 2).

Table 2
Descriptive statistics (x ± SD, n = 15) and results of ANOVA test
for measurements obtained from sepal samples of *Peganum harmala* (L.) collected from the study areas

Indicators	Mean ± SD, μm		ANOVA (Fisher's)			
	Aghdam (Aghdam Industrial Park area)	Zangilan (Bartaz village area)	F	df1	df2	p
Height of epidermis cells	37.30 ± 2.40	40.97 ± 2.32	18.176	1	28	2.1×10^{-4}***
Thickness of the outer periclinal walls of epidermis cells	13.69 ± 1.16	16.00 ± 1.67	19.206	1	28	1.5×10^{-4}***
Thickness of palisade-type parenchyma	154.07 ± 12.53	140.93 ± 18.42	5.213	1	28	3.0×10^{-2}*
Diameter of parenchyma cells around the bundles	42.32 ± 2.64	40.49 ± 2.19	4.237	1	28	4.0×10^{-2}*
Diameter of xylem vessels	10.17 ± 1.06	9.02 ± 1.20	7.768	1	28	9.4×10^{-3}**

Pedicel. Transverse sections of the pedicel, which supports the ripening fruits of *P. harmala*, were examined. Microscopic observations revealed that in specimens collected from the Aghdam region, notable accumulation processes occurred in parenchymatic and epidermal tissues, whereas in samples from the Zangilan region, pigmentation was more intensive in the stele (Fig. 10).

The epidermis covering the pedicel is overlain by a thick cuticular layer. The external periclinal walls of epidermal cells exhibited pronounced thickening, which was statistically confirmed to be more pronounced in the Zangilan specimens. Immediately beneath the epidermis, a subepidermal layer is present. This layer is characterized by the deposition of ergastic and constitutional substances within its cells. In the Aghdam specimens, these substances accumulated actively both in the subepidermal layer and in several epidermal cells.

Beneath the subepidermal layer lies the main portion of the cortex, composed of chlorenchyma. Microscopic analysis revealed intracellular inclusions within the chlorenchyma cells of the Aghdam pedicel samples, which are considered to be non-specific for the species. The remaining cortical region consists of isodiametric, chloroplast-free parenchyma cells, located adjacent to the sclerenchymatous ring. This ring completely encircles the stele. The stele exhibits a fascicular structure, with five large vascular bundles and five smaller vascular bundles situated between them, positioned slightly toward the cortex.

The central part of the stele is filled with pith parenchyma. In the Aghdam samples, cells of the pith parenchyma contained raphide-type, styloid-shaped, and other crystal forms. Overall, statistical analyses confirmed that the diameters of both the pith parenchyma and cortical parenchyma cells were larger in the Zangilan specimens (Table 3).

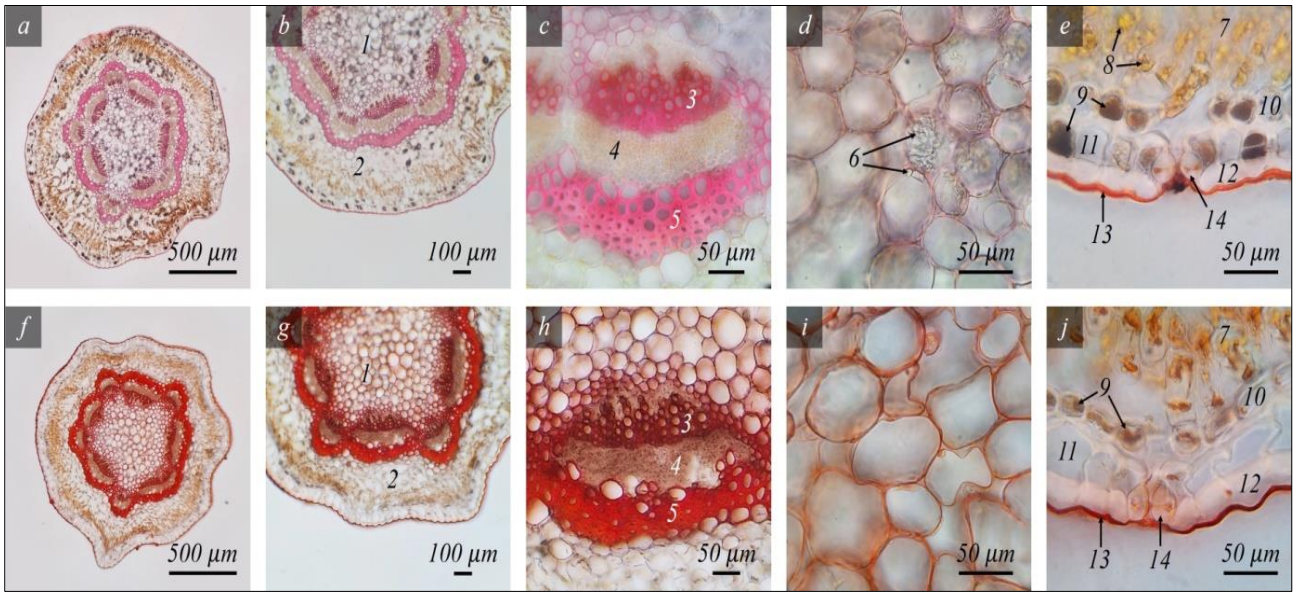

Fig. 10. Transverse sections of *Peganum harmala* (L.) pedicel samples from Aghdam (top row) and Zangilan (bottom row) (section thickness – 8 μm): *a*, *f* – general view of the section, *b*, *g* – a part of the section, *c*, *h* – structure of vascular bundles, *d*, *i* – pith parenchyma, *e*, *j* – peripheral part of the pedicel; *1* – pith, *2* – cortex, *3* – xylem, *4* – phloem, *5* – sclerenchyma, *6* – raphide-like and steloid crystals accumulated in pith cells, *7* – chlorenchyma, *8* – intracellular inclusion, *9* – accumulation of ergastic and constitutive substances in the epidermis and subepidermal layer, *10* – subepidermal layer, *11* – epidermis, *12* – thickened outer periclinal walls of epidermis cells, *13* – cuticle layer, *14* – guard cells

Table 3
Descriptive statistics (x ± SD, n = 15) and results of ANOVA test
for measurements obtained from pedicel samples of *Peganum harmala* (L.) collected from the study areas

Indicators	Mean ± SD, μm		ANOVA (Fisher's)			
	Aghdam (Aghdam Industrial Park area)	Zangilan (Bartaz village area)	F	df1	df2	p
Height of epidermis cells	46.41 ± 4.79	51.69 ± 7.19	5.615	1	28	2.4×10^{-2}*
Thickness of the outer periclinal walls of epidermis cells	14.28 ± 1.98	20.48 ± 3.28	18.302	1	28	1.0×10^{-3}**
Height of subepidermal cells	26.71 ± 2.33	24.45 ± 2.46	6.668	1	28	1.5×10^{-2}*
Thickness of cortex	214.26 ± 18.76	211.80 ± 27.49	0.081	1	28	7.7×10^{-1}
Diameter of cortical parenchyma cells	34.52 ± 3.48	40.75 ± 5.46	13.885	1	28	8.7×10^{-4}***
Thickness of sclerenchyma tissue	62.36 ± 5.90	62.65± 6.35	0.026	1	28	8.9×10^{-1}
Thickness of phloem	57.91 ± 4.55	50.88 ± 11.70	4.705	1	28	3.8×10^{-2}*
Diameter of xylem vessels	11.46 ± 1.72	11.29 ± 1.94	0.036	1	28	8.6×10^{-1}
Diameter of pith parenchyma cells	45.85 ± 3.89	52.62 ± 6.04	13.288	1	28	1.0×10^{-3}**

Leaf. Anatomical examination of *P. harmala* leaf samples collected from the two different regions revealed a largely similar structural organization. The leaves are of the isobilateral type. Along the central portion of the lamina, a single large vascular bundle is positioned in the midrib, accompanied by numerous smaller bundles distributed laterally. The epidermal cells enclosing the leaf are relatively large, with distinctly thickened outer periclinal walls. The epidermis is externally covered by a clearly visible cuticular layer. Stomata are present on both the adaxial and abaxial epidermis, indicating an amphistomatic leaf type. The leaves exhibit a thickened structure characteristic of xerophytic plants. Consistent with the species' adaptation to naturally arid and saline habitats, the mesophyll of the isobilateral leaf is dominated by palisade parenchyma (Sardarova, 2025c). A continuous and relatively thick layer of palisade cells, composed of two or more irregular rows of columnar cells, is located beneath the epidermis throughout the lamina. Beneath the stomata, substomatal air chambers are formed. A small amount of spongy parenchyma was also observed on the abaxial side of the leaf.

Statistical analyses demonstrated that the thickness of the palisade parenchyma was greater in the samples from the Aghdam site compared with those from Zangilan (Table 4). In these Aghdam specimens, large idioblasts were recorded within the palisade layer. Toward the inner mesophyll, around the vascular bundles, a zone of relatively isodiametric parenchyma cells occurs. Microscopic examination further revealed that, in cells adjacent to the palisade tissue – especially on the abaxial side – raphide-shaped calcium oxalate crystals were localized in specimens from both regions.

Previous studies have reported the absence of classical Kranz anatomy in *P. harmala*, which performs C_3 photosynthesis. However, as a result of adaptation to arid environments, structural modifications resembling Kranz-like organization were observed around the vascular system and within the mesophyll zone. Such Kranz-like cell arrangements, recorded for the first time under microscopic observations in this study, were present in both populations and may be regarded as an integral component of the water-saving mechanism (Voznesenskaya et al., 2017).

Table 4

Descriptive statistics (x ± SD, n = 15) and results of ANOVA test for measurements obtained from leaf samples of *Peganum harmala* (L.) collected from the study areas

Indicators	Mean ± SD (μm)		ANOVA (Fisher's)			
	Aghdam (Aghdam Industrial Park area)	Zangilan (Bartaz village area)	F	df1	df2	p
The height of the adaxial epidermis cells	43.18 ± 5.43	38.15 ± 4.72	7.324	1	28	1.1×10^{-2}*
Thickness of the outher walls of the adaxial epidermis cells	7.60 ± 0.73	7.16 ± 0.4 2	3.996	1	28	5.5×10^{-2}
The height of the palisade parenchyma tissue in the abaxial side	151.57 ± 8.31	143.40 ± 8.48	7.096	1	28	1.2×10^{-2}*
The height of the palisade parenchyma tissue in the adaxial side	194.44 ± 13.35	184. 80 ± 9.70	5.120	1	28	3.1×10^{-2}*
The height of the central bundles	142.65 ± 6.35	139.52 ± 6.98	1.649	1	28	2.0×10^{-1}
Diameter of the xylem vessels	16.34 ± 1.13	17.67 ± 1.57	7.036	1	28	1.3×10^{-2}*

Leaves, being directly exposed to the atmosphere, serve as the primary organs for the accumulation of airborne pollutants via aeration (Sahoo, 2024). Comparative analysis of samples from the contaminated area of the Aghdam Industrial Park and the ecologically clean area of Zangilan revealed the presence of non-specific inclusions localized in the vascular tissues and palisade parenchyma of the Aghdam specimens. Moreover, generalized parenchymatic inclusions were detected throughout all tissues. Microscopic analyses further confirmed the accumulation of crystals in the epidermal cells of leaves collected from Aghdam. In the same samples, the xylem elements of the vascular bundles exhibited significantly smaller diameters compared with those of the Zangilan specimens.

During the investigation, heterogeneous surface deposits of different origins were also observed on the leaf surface of *P. harmala*, particularly over and around the stomatal apparatus (Fig. 11). Morphologically, these deposits varied in size and shape and were identified not as intracellular inclusions but as exogenous particles of dust, mineral, or organic fragments. The presence of such deposits, functioning as an additional layer on the leaf surface, may influence stomatal activity and thus represents an ecologically relevant anatomical feature of considerable scientific importance.

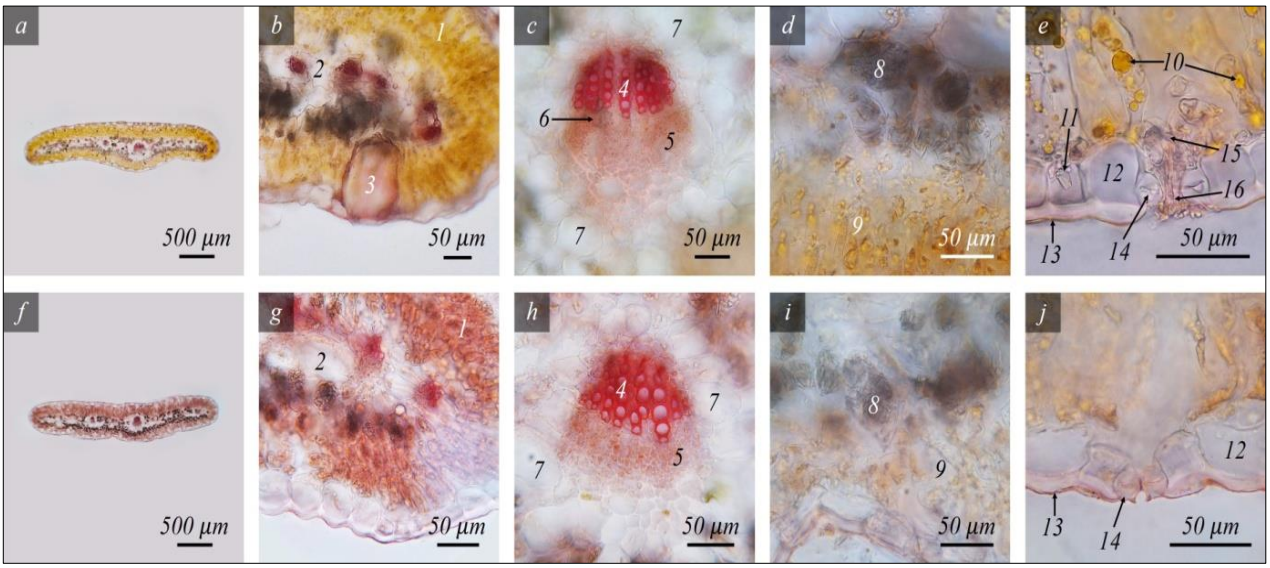

Fig. 11. Transverse sections of *Peganum harmala* (L.) leaf samples from Aghdam (top row) and Zangilan (bottom row) (section thickness – 9 μm): *a*, *f* – general view of the section, *b*, *g* – marginal part of the leaf, *c*, *h* – central bundle, *d*, *i* – degree of accumulation of accumulants in parenchymatous tissues, *e*, *j* – peripheral part of the leaf lamina; *1* – palisade parenchyma, *2* – parenchyma cells around the bundles, *3* – idioblast, *4* – xylem, *5* – phloem, *6* – nonspecific inclusion localization inside the bundle, *7* – Kranz-like cells, *8* – localization of raphide-type crystals at the boundary with palisade parenchyma, *9* – spongy parenchyma, *10* – intracellular inclusion, *11* – crystals in the epidermis, *12* – epidermis, *13* – cuticle layer, *14* – guard cells, *15* – non-homogeneous sediment, *16* – accumulations on the stomatal surface

Petiole. In transverse section, the petiole samples collected from the Aghdam site exhibited a relatively smooth upper surface, whereas those from the Zangilan site showed a slightly concave structure. The petiole is externally covered by an epidermis, beneath which lies a layer of prosenchymatous cells. In both ecotypes, the epidermis is overlain by a cuticular layer and bears stomata. Micrometric measurements revealed that the thickening of the outer periclinal walls of epidermal cells was less pronounced in the Aghdam samples (Table 5). In the same samples, brownish parenchymatic inclusions were recorded within the group of prosenchymatous cells. Furthermore, numerous drop-shaped intracellular inclusions were detected inside these cells under microscopic observation.

Towards the interior, the prosenchymatous zone transitions into a parenchymatous region surrounding the vascular bundles, composed mainly of isodiametric cells. The vascular bundles are relatively large in the central part and gradually decrease in size laterally. In both populations, the vascular bundles were well developed, consisting of abundant xylem elements, a distinct phloem region, and mechanical tissues. The sclerenchyma, as the main mechanical tissue, was found to be more prominently developed in the Zangilan specimens (Fig. 12).

Table 5

Descriptive statistics (x ± SD, n = 15) and results of ANOVA test
for measurements obtained from petiole samples of *Peganum harmala* (L.) collected from the study areas

Indicators	Mean ± SD, μm		ANOVA (Fisher's)			
	Aghdam (Aghdam Industrial Park area)	Zangilan (Bartaz village area)	F	df1	df2	p
Height of epidermis cells	40.75 ± 4.20	44.74 ± 3.60	7.832	1	28	9.1×10^{-3}**
Thickness of the outer periclinal walls of epidermis cells	8.53 ± 2.17	16.25 ± 4.72	17.340	1	28	1.1×10^{-3}**
Thickness of prosenchyma-type cell group	164.92 ± 28.75	137.27 ± 15.01	10.904	1	28	2.6×10^{-3}**
Diameter of parenchyma cells around the bundles	63.70 ± 8.05	56.90 ± 7.25	5.922	1	28	2.1×10^{-2}*
Diameter of xylem vessels	15.47 ± 2.75	15.01 ± 3.27	0.073	1	28	7.9×10^{-1}

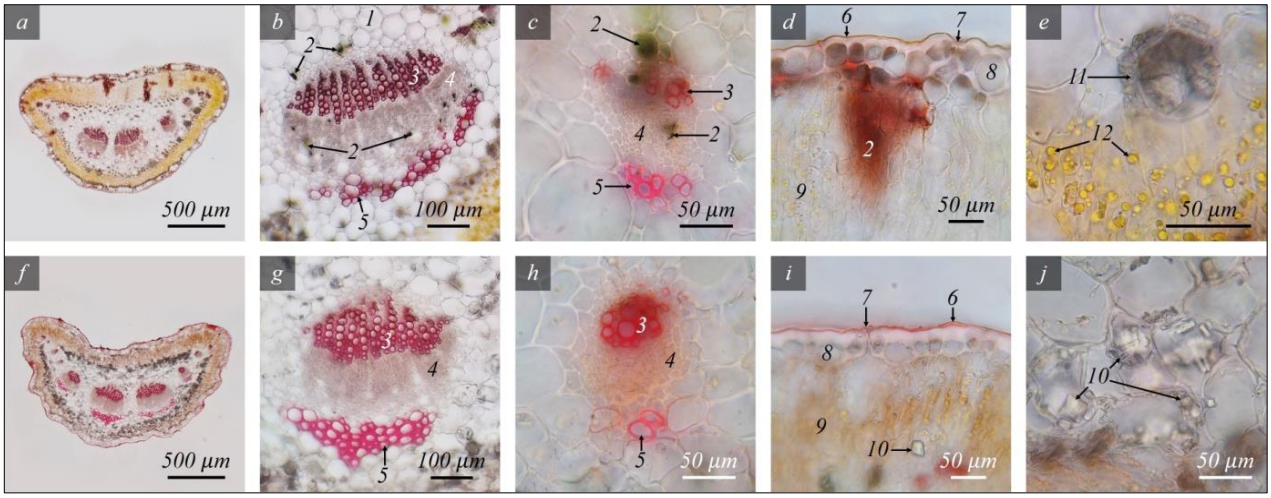

Fig. 12. Transverse sections of *Peganum harmala* (L.) petiole samples from Aghdam (top row) and Zangilan (bottom row) (section thickness – 8 μm): *a*, *f* – general view of the section, *b*, *g* – structure of large vascular bundles, *c*, *h* – characteristics of small vascular bundles, *d*, *i* – peripheral part of the petiole, *e*, *j* – degree of accumulation of accumulants in parenchymatous tissues; *1* – parenchyma area around the bundles, *2* – parenchymatous inclusions, *3* – xylem, *4* – phloem, *5* – sclerenchyma, *6* – cuticle layer, *7* – stomata, *8* – epidermis, *9* – prosenchyma-type cell group, *10* – prismatic, styloid, raphide-type and other forms of crystals, *11* – mass of ergastic substrances, *12* – intracellular inclusions

In petiole samples from the contaminated environment of Aghdam Industrial Park, small, dark-green parenchymatic inclusions were observed both within the xylem and phloem tissues of the vascular bundles and in the surrounding parenchymatous zones. Additionally, the cells bordering the prosenchymatous layer exhibited the accumulation of ergastic substances. This accumulation was more pronounced in the Zangilan samples, where the inclusions were represented by styloidal, prismatic, and raphide-type calcium oxalate crystals.

Stem. In both study sites, the stem stele was well developed and constituted the main part of the organ. Within the vascular system of the stele, the activation of the interfascicular cambium was evident. As a result, mechanical cells were formed, connecting the xylem tissues of the bundles into a continuous ring. These cells were identified as libriform fibers, providing mechanical support.

Through the exarch activity of the interfascicular cambium, newly formed phloem tissues merged with the primary phloem of the bundles, producing a complete phloem ring. Micrometric analysis confirmed that the thickness of the phloem was statistically greater in samples collected from the Aghdam site (Table 6).

Table 6

Descriptive statistics (x ± SD, n = 15) and results of ANOVA test
for measurements obtained from stem samples of *Peganum harmala* (L.) collected from the study areas

Indicators	Mean ± SD, μm		ANOVA (Fisher's)			
	Aghdam (Aghdam Industrial Park area)	Zangilan (Bartaz village area)	F	df1	df2	P
Height of epidermis cells	32.55 ± 2.10	35.19 ± 3.46	6.383	1	28	1.7×10^{-2}*
Thickness of the outer periclinal walls of epidermis cells	12.03 ± 1.14	13.44 ± 1.89	2.908	1	28	1.1×10^{-1}
Height of subepidermal cells	18.90 ± 3.30	14.24 ± 1.44	10.338	1	28	7.4×10^{-3}**
Cortex thickness	101.79 ± 7.84	113.28 ± 14.81	7.055	1	28	1.2×10^{-2}*
Diameter of cortical parenchyma cells	34.95 ± 2.73	32.98 ± 2.16	4.812	1	28	3.6×10^{-2}*
Thickness of sclerenchyma tissue	57.84 ± 12.34	58.24 ± 12.87	0.003	1	28	9.5×10^{-1}
Phloem thickness	67.97 ± 9.30	57.66 ± 8.23	10.324	1	28	3.3×10^{-3}**
Diameter of xylem vessels	18.02 ± 4.14	17.50 ± 2.54	0.091	1	28	7.6×10^{-1}
Diameter of pith parenchyma cells	92.80 ± 11.05	81.82 ± 10.46	7.816	1	28	9.2×10^{-3}**

The phloem region was surrounded by a ring of sclerenchymatous fibers, which in some places was interrupted by parenchymatic cells. Externally, the sclerenchymatous ring bordered one to two layers of isodiametric cortical parenchyma cells. In the Aghdam samples, dark intracellular inclusions were observed in some of these cortical parenchyma cells, as well as in certain cells located on both sides of the sclerenchyma ring and in the perimedullary zone of the pith. Additionally, in the cortical chlorenchyma of the Aghdam stems, orange-brown intracellular inclusions and large dark parenchymatic deposits were recorded. In contrast, in the Zangilan specimens, a limited accumulation of calcium oxalate crystals was observed in the cortical parenchyma cells.

The stem cortex was underlain by a subepidermal cell layer, which was externally covered by an epidermis. Micrometric measurements showed that subepidermal cells were relatively larger in the Aghdam samples, whereas epidermal cells were comparatively larger in the Zangilan samples. In both populations, ergastic and constitutional substances were accumulated in some epidermal and in many subepidermal cells. The outer, and to some extent,the inner periclinal walls of epidermal cells were thickened. The epidermis was covered with a thick cuticle, which also extended as a thin layer along the inner walls of guard cells and the substomatal cavities.

In both populations, crystals were recorded in the pith parenchyma cells. In stems from the Aghdam site, these were mainly raphide-shaped and small prismatic crystals. In some pith cells of these samples, porous-punctate structures were also detected under the microscope (Fig. 13). Such cells represent one of the most remarkable structural features of the *P. harmala* stem. Numerous small droplet-like or granular inclusions were visible within the cell lumen. This structure may have several explanations: these are large idioblast-type parenchyma cells specialized for secretion and storage. It is well known that the medicinal plant *P. harmala* contains idioblasts that accumulate alkaloids, essential oils, and other metabolites. Under light microscopy, these idioblasts appear as large, transparent cells containing fine granules and droplets, which corresponds with the present observations. In addition, in water-storing parenchyma cells of *P. harmala*, which grows in arid and semi-arid habitats, water can be accumulated as a reserve. In such cases, large parenchyma cells of the stem may contain abundant droplet-like inclusions within their vacuoles.

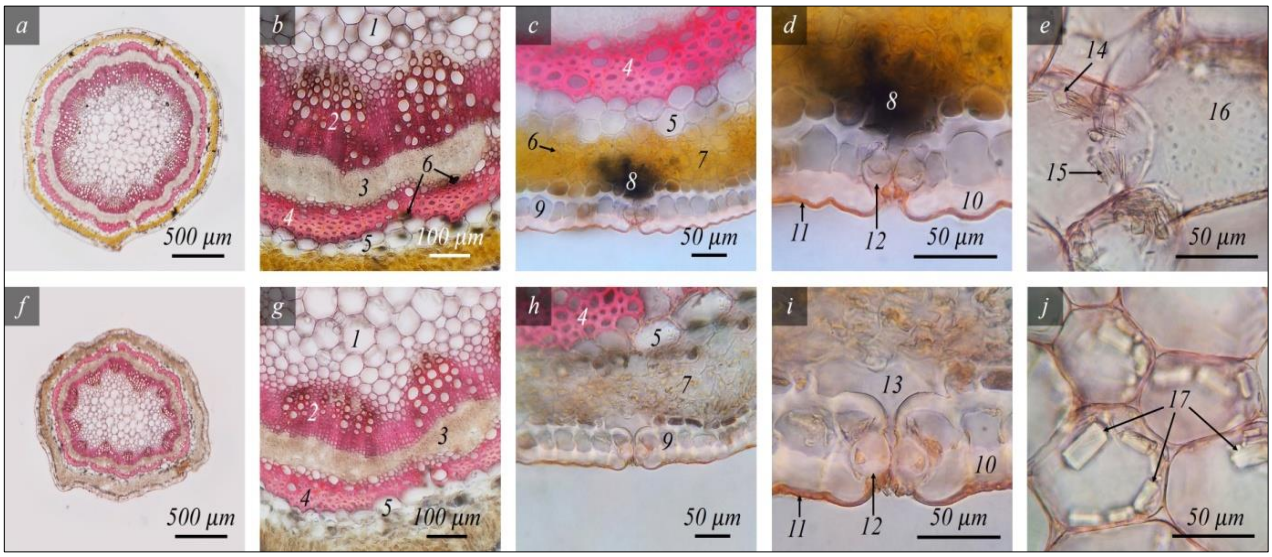

Fig. 13. Transverse sections of *Peganum harmala* (L.) stem samples from Aghdam (top row) and Zangilan (bottom row) (section thickness – 8 µm): *a*, *f* – general view of the section, *b*, *g* – a part of the stele, *c*, *h* – cortex, *d*, *i* – structural features in the epidermis and stomatal apparatus, *e*, *j* – level of accumulation in pith parenchyma cells; *1* – pith, *2* – xylem, *3* – phloem, *4* – sclerenchyma, *5* – cortical parenchyma cells, *6* – intracellular inclusions, *7* – chlorenchyma, *8* – parenchymatous inclusions, *9* – epidermis, *10* – thickened outer periclinal walls of epidermis cells, *11* – cuticle, *12* – guard cells, *13* – sub-stomatal cavity, *14* – prismatic crystals, *15* – raphide-type crystals, *16* – idioblast (porous-dot structured), *17* – styloid crystals

The small punctate structures observed within these cells may also represent the initial stages of crystal formation (e.g., calcium oxalate crystals) or vacuolar accumulations of secretory products. Thus, these cells should not be regarded as ordinary parenchyma, but rather as idioblast-type parenchyma cells with specialized storage or secretory functions. Such a structure can be ecologically explained by the species' drought resistance and pharmacobotanically by its production of alkaloid-containing secretory metabolites. The idioblastic nature of these cells allows certain functional assumptions; however, precise confirmation requires molecular analysis of their intracellular compounds.

In the Zangilan samples, calcium oxalate crystals in the pith were predominantly of the styloidal type, although a few raphide-shaped crystals were also recorded.

Root. Transverse sections of roots collected from different sites revealed structural variations. The central region of the root was occupied by xylem tissue, composed of xylem vessels interspersed with libriform fibers. Statistical analysis indicated that the overall diameter of xylem vessels was smaller in samples collected from the Aghdam site. In these samples, secondary wall thickening of both xylem vessels and libriform fibers was more pronounced. The xylem was divided by a thin parenchyma layer into a large central portion and smaller lateral portions. The xylem was surrounded by a multilayered cambium. Microscopic analysis of roots from the Zangilan site showed that the exarch activity of the cambium led to the formation of multiple concentric layers of sclerenchyma and phloem toward the cortex (Fig. 14). The phloem cells in these layers were relatively large. In contrast, in Aghdam samples, sclerenchyma fibers formed a single mechanical ring around the phloem, exhibiting more intensive lignification and thicker cell walls.

Statistical measurements of cortical parenchyma indicated that cells were larger in plants from the Zangilan site. Within these cells, accumulations of ergastic substances were observed. In both site samples, these ergastic inclusions are likely to represent stored starch. Druse crystals were also observed in the cortical parenchyma of roots from the Zangilan site.

The cortex was externally covered by a periderm. Although the periderm was thicker in the Aghdam samples, the individual periderm cells were larger in the Zangilan samples (Table 7). Microscopic observations revealed that roots from plants growing in the contaminated environment of Aghdam Industrial Park exhibited remnants of tissues formed at an early stage on the outer side of the periderm. These dead tissue remnants contained sclerenchyma fibers, cells with accumulated ergastic substances, and parenchymatic inclusions.

Table 7
Descriptive statistics (x ± SD, n = 15) and results of ANOVA test
for measurements obtained from root samples of *Peganum harmala* (L.) collected from the study areas

Indicators	Mean ± SD, µm		ANOVA (Fisher's)			
	Aghdam (Aghdam Industrial Park area)	Zangilan (Bartaz village area)	F	df1	df2	P
The height of the periderm cells	16.63 ± 1.90	19.68 ± 2.86	11.869	1	28	1.8×10^{-3}**
Diameter of the cortex parenchyma cells	31.98 ± 6.66	43.05 ± 6.08	22.648	1	28	5.3×10^{-5}***
Diameter of the xylem vessels	53.84 ± 7.62	70.68 ± 12.98	18.781	1	28	1.7×10^{-4}***

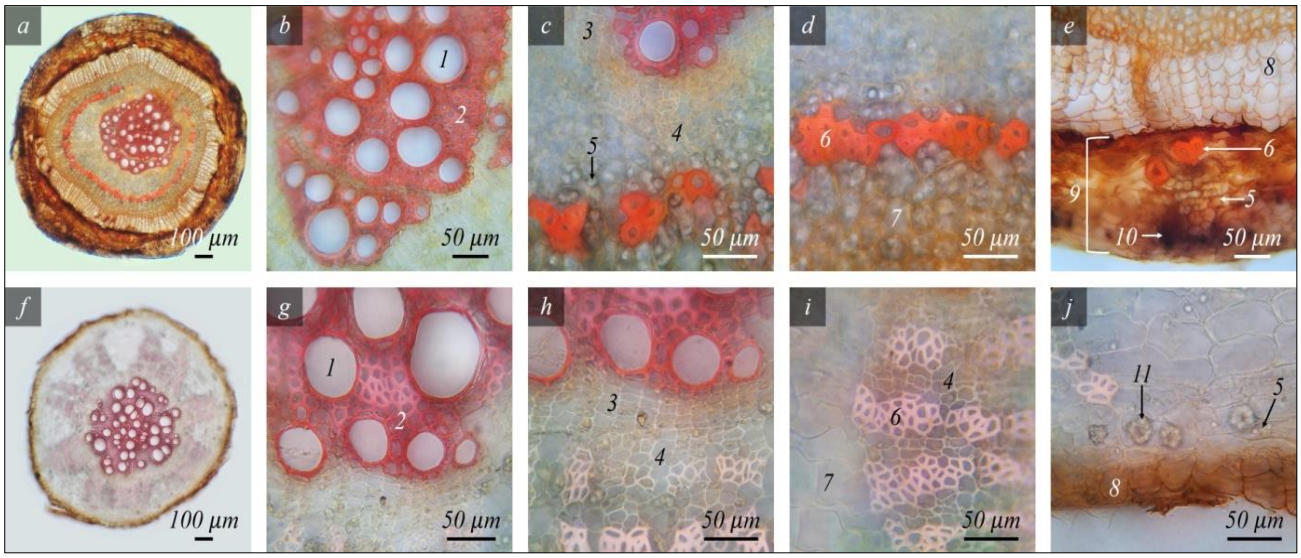

Fig. 14. Transverse sections of *Peganum harmala* (L.) root samples from Aghdam (top row) and Zangilan (bottom row) (section thickness – 8 µm): *a, f* – general view of the section, *b, g* – structure of the xylem, *c, h* – cambium and phloem area, *d, i* – development level of sclerenchyma tissue, *e, j* – cortex and protective tissues; *1* – xylem vessel, *2* – libriform fibers, *3* – cambium, *4* – phloem, *5* – ergastic substances, *6* – sclerenchyma, *7* – cortical parenchyma, *8* – periderm, *9* – supernumerary periderm, *10* – parenchymatous inclusions, *11* – druse crystals

Discussion

The anatomical alterations observed in the leaf tissues of the medicinally valuable species *P. harmala* as a result of phytocontamination represent a clear indicator of the stress induced by ecological pollution factors in the ecosystem. The presence of dark inclusions scattered across the leaf lamina indicates local intra- and intercellular accumulation of substances, particularly those associated with heavy metals. The abundance of small, dark yellow droplet-like inclusions within the palisade parenchyma cells may be interpreted as evidence of disrupted intracellular metabolic processes and the activation of detoxification-related defense mechanisms (Nouha et al., 2024). Granular structures and crystal inclusions (e.g., oxalate crystals or proteinaceous complexes) recorded in epidermal cells are associated with the accumulation of phytochemical components, which can be regarded as an adaptive response of the plant to xenobiotic substances (Tütüncü Konyar et al., 2014). One of the most striking consequences of ecological stress is reflected in the stomatal apparatus. The complete occlusion of the stomatal pore by undefined deposits, along with the separation of the guard cells, may lead to impairment of stomatal function, thereby severely restricting gas exchange and transpiration. These findings demonstrate that the examined *P. harmala* specimens are highly exposed to phytocontamination.

In the adaxial mesophyll of *P. harmala* leaves grown under phytocontamination, abnormally enlarged parenchymatic cells were observed between the columnar parenchyma cells. One hypertrophied cell, with a width nearly equal to four columnar cells, exerted mechanical pressure on the overlying epidermal layer, resulting in pronounced thinning and deformation. The emergence of such structures can be linked to cytotoxic stress induced by heavy metals, and these cells may have formed as a result of stress-induced idioblast differentiation. According to recent studies, these types of cells can function as localized detoxification sites by sequestering excess metal ions and metabolites, thereby mitigating widespread tissue damage. The sporadic formation and large size of these cells are likely associated with disturbances in cell division and differentiation processes, triggered by oxidative signaling and hormonal imbalance under stress conditions. These observations are consistent with anatomical plasticity and adaptive cellular reorganization mechanisms in plants subjected to environmental pollution. Consequently, the anatomical changes detected in *P. harmala* highlight its ecological significance as a bioindicator and phytoremediator species. The inclusions and crystal structures identified can serve as valuable microscopic markers for monitoring pollution.

For the first time, a Kranz-like isobilateral xeromorphic structure was identified in the leaves of *P. harmala*. In specimens collected from both unpolluted and phytocontaminated environments, large parenchymatic cells were found surrounding the vascular bundles. Although the circular organization of these cells around the bundles morphologically resembles Kranz anatomy, no evidence of functional activity related to the C_4 photosynthetic pathway was confirmed in this study. Only the visual-anatomical features of these tissues were analyzed as the focus of this investigation. It may be assumed that such structures serve functions such as minimizing water loss, enhancing the efficiency of transport, and facilitating adaptation to stress, and thus represent an important anatomical adaptation conferring resilience to arid and polluted habitats. While the bundle sheath structure morphologically resembles Kranz anatomy, additional physiological and biochemical analyses are recommended to confirm its functional classification and its relation to a specific Kranz type. The presence of well-developed palisade parenchyma on both adaxial and abaxial surfaces, poorly developed spongy tissue, and radially arranged Kranz-like cells around the vascular system suggests the possibility of an intermediate C_3–C_4 photosynthetic type. Furthermore, thickened epidermis, high cell density, and variability in the stomatal apparatus reflect xerophytic strategies that enhance ecological resilience in arid and saline habitats. These anatomical features not only support adaptation to abiotic stress but may also enhance the biosynthetic potential for bioactive compounds. The findings highlight the physiological and anatomical plasticity of *P. harmala* and emphasize the necessity of

further investigation of this species as a novel eco-anatomical model. The conducted investigations revealed that in *P. harmala*, a medicinally significant species, root tissues of individuals growing in ecologically contaminated habitats exhibited substantial anatomical modifications. In particular, the denser arrangement and reduced size of xylem elements within the central cylinder can be interpreted as an adaptive defensive response (Glavač et al., 2017; Khan et al., 2023). These alterations were accompanied by intensified lignification and sclerification in xylem vessels and libriform fibers, which may serve to partially restrict the translocation of heavy metals and other contaminants into the transpiration system. The partitioning of the xylem into large central and smaller lateral regions by parenchymatous bands, along with the localization of inclusions within these areas, indicates a strategy of isolating potentially harmful substances in defined compartments.

The weak development of the cambium and incomplete formation of the sclerenchyma–phloem complex further suggest that long-term stress exerts an inhibitory effect on meristematic activity. The dense and irregular structure of phloem cells may reflect impaired metabolic exchange (Hlihor et al., 2022). Small groups of sclerenchyma fibers distributed around the phloem can be regarded as an adaptive mechanism aimed at maintaining structural support. Enhanced sclerification and secondary thickening of sclerenchymatous fiber walls highlight the influence of ecological stressors – particularly heavy metals – on lignification and cell wall modification processes. Such responses simultaneously strengthen the mechanical stability of the root system, thereby enhancing its resistance under stress conditions.

In the cortex, the reduced cell size and accumulation of a larger amount of ergastic inclusions demonstrate intensified detoxification and storage processes. The development of a thick, multi-layered periderm represents one of the key structural barriers against ecological stress, providing both mechanical and chemical protection. The persistence of residual tissues, sclerenchyma fibers, and inclusion-rich cells within the periderm indicates that newly formed protective layers originate from the phloem–cortex boundary at later developmental stages.

Peripheral alterations in the roots of plants collected from polluted habitats further support this adaptive interpretation. Degraded epidermal layers gave rise to protective tissues functioning as a mechanical barrier between the plant and its environment. In these samples, supernumerary periderm formation was detected above the primary periderm. Parenchymatous cells beneath this layer exhibited protoplasmic coagulation and reduced intercellular spaces, pointing to tissue compaction in response to stress. The presence of dark pigments within these cells can be linked to the sequestration of heavy metals and other contaminants (Asgari Lajayer et al., 2017). Such features are indicative of morpho-anatomical adaptation, reflecting the plant's capacity to filter and accumulate toxic substances.

The coexistence of sclerenchyma cells with starch-rich parenchyma in this peripheral zone suggests the emergence of a composite adaptive tissue under contaminated conditions. This dual structural-functional system not only restricts diffusion of toxicants but also ensures energy supply during prolonged stress periods.

Overall, the findings demonstrate that *P. harmala* has evolved a suite of structural and physiological defense mechanisms against ecological contamination. These responses, including lignification, compartmentalization of inclusions, and periderm thickening, represent specialized adaptations that enable the plant to withstand heavy metal exposure. Consequently, *P. harmala* may be regarded as a promising model species for ecological monitoring.

Microscopic analyses of the generative organs of *P. harmala* revealed that in seed samples collected from both sites, endosperm cells were rich in storage compounds, confirming their role as an energy reservoir essential for normal seed development and germination. In the sample collected from the Aghdam industrial park, the intense localization of non-specific inclusions in endotestal cells may reflect anatomical alterations associated with soil and air contamination in this area. In contrast, the reddish coloration of tissues in the Zangilan sample can be attributed to the abundance of anthocyanins and other phenolic compounds, representing an adaptive response to environmental stressors. In the sepal organ, the presence of idioblasts surrounding the central vascular bundle in the Aghdam sample suggests secretory activity or the accumulation of defensive metabolites (alkaloids, crystalline calcium oxalate, phenolics). Dark deposits and prismatic crystals observed in the epidermis and at the boundary of the palisade parenchyma indicate the activation of specialized detoxification mechanisms against heavy metals and other toxic components in contaminated habitats.

In the pedicel of the Aghdam sample, dark-colored deposits accumulated in epidermal and subepidermal cells may be interpreted as metabolic products associated with the accumulation of secondary metabolites (polyphenols, flavonoids) and heavy metal complexes under stress conditions (Yadav et al., 2021). The presence of needle-shaped and rod-shaped crystals in the pith further supports this interpretation. By contrast, in the Zangilan sample, the more intense staining of the cuticle, sclerenchyma, xylem, and pith cell walls indicates more active lignification and thickening processes, which may enhance mechanical strength and resistance to water stress.

In the petiole of the Aghdam sample, dark deposits and large crystalline precipitates detected in vascular and palisade parenchyma can be regarded as forms of ecotoxin (heavy metals, salts) storage. The accumulation of dark deposits in the epidermis likewise indicates an increase in secondary metabolites, particularly phenols and tannins, associated with contamination. In the Zangilan samples, however, the predominance of prismatic, styloid, amorphous, and especially raphide-type crystals, together with the more active sclerenchyma, reflects structural adaptations to mechanical and hydric stresses in the environment. In the stem of the Aghdam sample, the occurrence of large dark spots in the chlorenchyma is most likely linked to the accumulation of anthocyan pigments or heavy metal-phenol complexes. The greater abundance of dark deposits in epidermal and subepidermal cells indicates intensified defense responses under contamination, or unknown intracellular accumulations in phytocontaminated tissues. In the pith of the Aghdam sample, the abundance of needle-shaped, prismatic, and irregularly shaped crystals, along with "punctate-structured" cells, demonstrates the plant's ability to form specialized structural adaptations to the polluted environment. In contrast, the predominance of rod-shaped crystals in the Zangilan sample confirms the prevalence of adaptive crystallization processes.

Overall, the findings suggest that in the Aghdam industrial park samples, contamination stress is associated with the proliferation of idioblasts, the formation of dark deposits and large crystalline inclusions, and the accumulation of dark pigments in chlorenchyma. In the Zangilan samples of *P. harmala*, however, the diversity of prismatic, raphide, and amorphous crystals, together with active lignification of sclerenchyma and cell walls, is particularly notable. These contrasts highlight the site-specific ecological impacts on plant anatomy and their diagnostic value in ecological anatomy. Importantly, the study also revealed the occurrence of unknown inclusions in diverse localization forms (intracellular, intercellular, and parenchymatic) across both vegetative and generative organs. Their non-specific distribution suggests that they can be visualized primarily at the anatomical level and require classical histological techniques for accurate detection.

The more intensive occurrence of such inclusions in samples from contaminated ecosystems suggests their possible interpretation as an ecotoxicological response mechanism to anthropogenic stress factors. These accumulations may play a role in detoxification by neutralizing or sequestering heavy metals, toxins, or stress-induced metabolites under ecological pressure (Asiminicesei et al., 2024). This is considered one of the key indicators of plant resilience and adaptive capacity. From a pharmacobotanical perspective, these findings are of particular relevance, since the presence of such structures in medicinal plant raw material may directly influence the content, quality, and toxicological safety of bioactive compounds. Thus, integrating anatomical observations with phytochemical and toxicological analyses is essential for updating pharmacopoeial standards. Ultimately, the study demonstrates that the visualization of unknown inclusions represents not only a contemporary direction in ecological anatomy but also provides a valuable tool for assessing plant adaptation potential

under anthropogenic stress, monitoring ecosystem health, and evaluating the quality of medicinal plant resources.

Koyuncu et al. (2008), in their study of leaf anatomy, reported that the leaf epidermis is covered by a cuticle. This observation is consistent with our findings. However, our analysis further revealed that in *P. harmala* individuals growing in the Aghdam Industrial Park area, the cuticular layer was relatively thickened. Foreign authors have also noted that the leaves of *P. harmala* are amphistomatic, which was confirmed in our study for both ecotypes examined.

Seilkhan et al. (2019), in their investigation of the vegetative organs of *P. harmala*, demonstrated the formation of a thick periderm in the root. Our study similarly showed pronounced peridermal development in roots of plants from the Aghdam ecosystem. Moreover, in these roots, we identified a parenchyma layer external to the periderm, containing sclerenchyma elements and ergastic substances. While previous authors indicated that the root cortex is composed of a ring-shaped sclerenchyma and parenchyma, our findings only partially agree. Specifically, in Aghdam plants, sclerenchyma fibers form a ring within the cortex, whereas in roots of plants from Zangilan, the cortex exhibits a layered arrangement of phloem-sclerenchyma structures. Earlier reports also mentioned the presence of a uniseriate cambium between xylem and phloem; however, our observations revealed that in both ecotypes, the cambium is multiseriate.

El Hasnaoui et al. (2023) conducted a hydroponic experiment to examine the response of *P. harmala* plants collected from polluted and unpolluted sites to lead and zinc stress. For 15 days, plants were exposed to metal salts, resulting in a reduction of aboveground biomass. Root damage under metal stress was more pronounced in plants originating from clean habitats. The authors reported that photosynthetic activity did not significantly differ under stress, suggesting that chlorophyll synthesis is not impaired by metal exposure. They also emphasized that proline and antioxidants were synthesized at higher levels under stress, with plants from clean habitats showing stronger metabolic responses. The study concluded that plants from polluted habitats were more resistant to metal stress, while metal accumulation was stronger in plants from unpolluted habitats.

This interpretation is highly relevant and timely. The higher accumulation observed in clean-habitat plants may be explained by their ongoing acclimatization to new environmental conditions, rendering them more sensitive to stress. In contrast, in our study, *P. harmala* samples collected from both the ecologically polluted Aghdam Industrial Park and the ecologically clean Zangilan ecosystem were already fully naturalized to their environments. Consequently, their metabolic processes and the accumulation of non-specific inclusions were maintained as adaptive traits.

Conclusion

This study, for the first time, carried out a comparative visual analysis of unidentified intracellular and intercellular deposits, as well as diagnostic anatomical structures at both the cellular and tissue levels, in the vegetative and generative organs of *P. harmala* collected from both contaminated and ecologically clean sites. The results demonstrate that these structures represent reliable indicators of morpho-anatomical adaptations to diverse ecological conditions. Thus, the study contributes novel data to the fundamental field of plant anatomy, while simultaneously advancing contemporary research directions in ecological anatomy.

Specific anatomical structures – such as cell size and shape, compact parenchymatic organization in assimilatory tissues, stomatal localization patterns, and the distribution of inclusions – were recorded for the first time as ecosystem-specific markers in both vegetative and generative organs from contrasting environments. These observations not only reflect the morpho-anatomical adaptation strategies of the species but also hold practical and scientific significance, particularly for the evaluation of medicinal plant raw material quality, biomonitoring applications, and the development of ecological-anatomical indices. Consequently, this investigation is considered a primary and innovative source of information for both plant anatomy and ecological anatomy as emerging scientific disciplines.

In seeds of *P. harmala* collected from contaminated sites, the inclusions observed are most likely exogenous intracellular deposits. These intracellular inclusions clearly reflect the influence of environmental factors as anatomical-botanical indicators. Microscopic analyses revealed tissue-level accumulations of deposits with no defined chemical composition, which within the framework of modern botany and plant anatomy may be classified as endogenic and exogenic intracellular inclusions. Further research is required to clarify their origin. To elucidate the provenance and mechanisms of these inclusions detected in the internal tissues of *P. harmala* collected from contaminated habitats, ecological-toxicological, phytochemical, isotopic, biochemical, physiological, and molecular investigations are recommended.

In the abaxial parenchyma of *P. harmala* leaves under phytocontaminated conditions, stress-induced idioblasts with hypertrophied cells were observed, indicating adaptive defense mechanisms such as localized detoxification and anatomical plasticity. The presence of an isobilateral xeromorphic structure with Kranz-like features, along with intracellular inclusions, confirms the high ecological adaptability of the species to arid and polluted environments. This, in turn, enhances the value of *P. harmala* as a bioindicator and a sustainable pharmacological plant resource. In root tissues, periderm thickening, sclerenchymatization, lignification, and the occurrence of unidentified inclusions were interpreted as adaptive structural modifications. For the first time, abnormal periderm thickening and the persistence of early tissue remnants – interpreted as ecological press differentiation in the plant kingdom – were documented as novel findings. The development of modified sclerenchymatic and starch-bearing parenchyma cells in the outer periderm layers indicates dual adaptation strategies, ensuring both mechanical support and energy storage.

The detection of non-specific intracellular inclusions in contaminated *P. harmala* samples, together with associated anatomical modifications at the tissue level, highlights the necessity of conducting phytochemical research to assess their pharmacological quality under polluted environmental conditions. Overall, this study provides the first evidence that *P. harmala*, a medicinally valuable species, responds to environmental contamination with structural adaptations, reinforcing its potential as both a bioindicator and a candidate phytoremediator. Considering current international research priorities, including anthropogenic ecosystem dynamics and global climate change, the ecological-anatomical data presented here may serve as valuable biological markers within multidisciplinary resource platforms.

This research did not receive any specific grant from funding agencies in the public, commercial, or not-for-profit sectors.

The authors declare that they have no known competing financial interests or personal relationships that could have appeared to influence the work reported in this paper.

References

Ahmad, I., Shamsi, L., Hameed, M., Fatima, S., Ahmad, F., Aqeel Ahmad, M. S., Ashraf, M., Javaid, A., & Sultan, M. A. (2021). Micro-morphological response of some native dicotyledonous species to particulate pollutants emitted from stone crushing activities. Environmental Science and Pollution Research, 28, 25529–25541.

Ait Elallem, K., Ben Bakrim, W., Ennoury, A., Metougui, M. L., Yasri, A., & Boularbah, A. (2022). Germination parameters and responses of antioxidant enzymatic activities of two medicinal plants (*Peganum harmala* L. and *Origanum majorana* L.) under heavy metal stress. Journal of Soil Science and Plant Nutrition, 22, 3942–3957.

Akhtar, M. F., Raza, S. A., Saleem, A., Hamid, I., Baig, M. M. F. A., Sharif, A., Sohail, K., Javaid, Z., Saleem, U., & Rasul, A. (2022). Appraisal of anti-arthritic and anti-inflammatory potential of folkloric medicinal plant *Peganum harmala*. Endocrine, Metabolic and Immune Disorders – Drug Targets, 22(1), 49–63.

Asgari Lajayer, B., Ghorbanpour, M., & Nikabadi, S. (2017). Heavy metals in contaminated environment: Destiny of secondary metabolite biosynthesis, oxidative status and phytoextraction in medicinal plants. Ecotoxicology and Environmental Safety, 145, 377–390.

Asiminicesei, D. M., Fertu, D. I., & Gavrilescu, M. (2024). Impact of heavy metal pollution in the environment on the metabolic profile of medicinal plants and their therapeutic potential. Plants, 13(6), 913.
Basahi, M. A. (2023). Interactions in germination responses to salinity, temperature and light in the desert shrub African rue (*Peganum harmala* L.). Applied Ecology and Environmental Research, 21(1), 85–98.
Benlarbi, F., & Chaachouay, N. (2025). Wild rue (*Peganum harmala* L. Nitrariaceae). In: Chaachouay, N., Azeroual, A., & Zidane, L. (Eds.). Comprehensive guide to hallucinogenic plants. CRC Press, Boca Raton. Pp. 272–282.
Bozdağ, B., Kocabaş, O., & Özdemir, C. (2016). A new staining method for hand-cut in plant anatomy studies. Marmara Pharmaceutical Journal, 20(2), 184–190.
Chamberlain, C. J. (2020). Methods in plant histology. Forgotten Books, London.
Čiamporová, M., Nadubinská, M., Barnásová, V., Ďurišová, E., Zelinová, V., Horak, O., Gruber, D., & Lichtscheidl, I. K. (2021). Structural traits of leaf epidermis correspond to metal tolerance in *Rumex acetosella* populations growing on metal-contaminated soils. Protoplasma, 258, 1277–1290.
Collin, K., Baskar, A., Geevarghese, D. M., Syed Ali, M. N. V., Bahubali, P., Choudhary, R., Lvov, V., Tovar, G. I., Senatov, F., Koppala, S., & Swamiappan, S. (2022). Bioaccumulation of lead (Pb) and its effects in plants: A review. Journal of Hazardous Materials Letters, 3, 100064.
Criswell, S., Gaylord, B., & Pitzer, C. R. (2025). Histological methods for plant tissues. Journal of Histotechnology, 48(1), 58–67.
Da Silva, C. J., de Lima, L. H. F., de Paiva, P. M., Maia, L. M., de Oliveira Rocha, R. E., de Souza, P. T. D., & Carvalho, D. A. C. A. (2020). An inexpensive and environmentally friendly staining method for semi-permanent slides from plant material probed using anatomical and computational chemistry analyses. Rodriguésia, 71, e01662018.
Doskaliyev, A., Seidakhmetova, R., Tutai, D. S., Goldaeva, K., Surov, V., & Adekenov, S. (2021). Alkaloids of *Peganum harmala* L. and their pharmacological activity. Open Access Macedonian Journal of Medical Sciences, 9(A), 766–775.
El Hasnaoui, S., Diallo, A. D., Wandan, N., & Colin, F. (2023). Lead and zinc tolerance and accumulation in metallicolous and non-metallicolous populations of *Peganum harmala* L.: Potential use in phytostabilization. Bioremediation Journal, 28(3), 302–324.
Engin, H., Kuzucu, F. C., & Gökbayrak, Z. (2024). Research on the use of different staining techniques in microscopic examination and imaging of wood cuttings. ÇOMÜ Journal of Agricultural Faculty, 12(1), 108–120.
Gao, Z., Mu, Y., Chen, F., He, L., Li, X., Li, J., Ding, K., Cu, Y., Mu, C., & Rasheed, A. (2025). Effects of pericarp removal and different germination conditions on seed germination and saline-alkali tolerance of *Amorpha fruticosa*. Turkish Journal of Botany, 49(1), 40–51.
Glavač, N. K., Djogo, S., Ražić, S., Kreft, S., & Veber, M. (2017). Accumulation of heavy metals from soil in medicinal plants. Archives of Industrial Hygiene and Toxicology, 68(3), 236–244.
Han, Y., Lee, J., Haiping, G., Kim, K. H., Wanxi, P., Bhardwaj, N., Oh, J. M., & Brown, R. J. C. (2022). Plant-based remediation of air pollution: A review. Journal of Environmental Management, 301, 113860.
Hlihor, R. M., Roșca, M., Hagiu-Zaleschi, L., Simion, I. M., Daraban, G. M., & Stoleru, V. (2022). Medicinal plant growth in heavy metals contaminated soils: Responses to metal stress and induced risks to human health. Toxics, 10(9), 499.
Ibadullayeva, S. J. (2024). Traditional folk medicine of Azerbaijanis. Savad, Baku.
Jambor, H., Antonietti, A., Alicea, B., Audisio, T. L., Auer, S., Bhardwaj, V., Burgess, S. J., Ferling, I., Gazda, M. A., Hoeppner, L. H., Ilangovan, V., Lo, H., Olson, M., Mohamed, S. Y., Sarabipour, S., Varma, A., Walavalkar, K., Wissink, E. M., & Weissgerber, T. L. (2021). Creating clear and informative image-based figures for scientific publications. PLoS Biology, 19(10), e3001161.
Karim, A., Naz, S., Ahmad, W., Bano, N., Zubair, M., Gul, S., Ramzan, A., Ali, Z., Waqas, K., Alahmadi, T. A., & Ansari, M. J. (2024). Biochemical attributes of zinc-induced stress on *Cicer arietinum*. Pakistan Journal of Botany, 56(5), 1671–1678.
Khan, I. U., Qi, S.-S., Gul, F., Manan, S., Rono, J. K., Naz, M., Shi, X.-N., Zhang, H., Dai, Z.-C., & Du, D.-L. (2023). A green approach used for heavy metals 'phytoremediation' via invasive plant species to mitigate environmental pollution: A review. Plants, 12(4), 725.
Koyuncu, O., Öztürk, D., Potoğlu Erkara, İ., & Kaplan, A. (2008). Anatomical and palynological studies on economically important *Peganum harmala* L. (Zygophyllaceae). Biological Diversity and Conservation, 1(1), 108–115.
Krzesłowska, M., Goliński, P., Szostek, M., Mocek-Płóciniak, A., Drzewiecka, K., Piechalak, A., Ilek, A., Neumann, U., Timmers, A. C. J., Budzyńska, S., Mleczek, P., Suski, S., Woźny, A., & Mleczek, M. (2021). Morphology and physiology of plants growing on highly polluted mining wastes. In: Prasad, R. (Ed.). Phytoremediation for environmental sustainability. Springer, Singapore. Pp. 151–200.
Li, L. (2024). *Peganum harmala* L.: A review of botany, traditional use, phytochemistry, pharmacology, quality marker, and toxicity. Combinatorial Chemistry and High Throughput Screening, 27(6), 797–822.
Mahdavian, K. (2022). Investigation of the metal bioremediation ability of two populations of *Peganum harmala*. Avicenna Journal of Environmental Health Engineering, 9(1), 18–24.
Muszyńska, E., Rossini-Oliva, S., & Wiszniewska, A. (2023). Costs and trade-offs in plant adaptation and acclimation to metals. Frontiers in Plant Science, 14, 1245426.
Nouha, K., Mounira, G. M., Lamia, H., Shahhat, I., Mehrez, R., & Arbi, G. (2024). Physiological and biochemical responses in Mediterranean saltbush (*Atriplex halimus* L., Amaranthaceae Juss.) to heavy metal pollution in arid environment. Pakistan Journal of Botany, 56(5), 1717–1726.
Peterson, R. L., Peterson, C. A., & Melville, L. H. (2008). Teaching plant anatomy through creative laboratory exercises. NRC Press, Ottawa.
Qurbanov, E. M. (2024). Azərbaycanın bitki örtüyü [Vegetation of Azerbaijan]. Elm, Baku (in Azerbaijani).
Sahoo, M. (2024). Exploring the role of plants in bio-remediation: Harnessing nature's clean-up agents. International Journal of Multidisciplinary Approach Research in Science, 2(2), 726–732.
Sardarova, A. S. (2024). The anatomical characteristics of the vegetative and generative organs of the medicinal *Silybum marianum* L. spread in the mountainous region of the Lesser Caucasus. Advances in Biology and Earth Sciences, 9(3), 381–388.
Sardarova, A. S. (2025a). Comparative ecological anatomical characteristics of generative and vegetative organs of the medicinally important plant *Fragaria vesca* L. (Rosaceae Juss.) under *in situ* and *ex situ* conditions. Transactions of the Institute of Molecular Biology and Biotechnologies, 9(1), 17–37.
Sardarova, A. S. (2025b). Comparative ecological anatomical study of the structural adaptation of the medicinally important plant *Salvia nemorosa* L. under *in situ* and *ex situ* conditions. Acta Botanica Caucasica, 4(2), 81–100.
Sardarova, A. S. (2025c). Ecological and anatomical characteristics and tolerance of *Salsola nodulosa* Iljin and *Zygophyllum fabago* L. species under ecological pressures in and saline ecosystems. Acta Botanica Caucasica, 4(1), 106–123.
Sardarova, A., & Ibadullayeva, S. (2025). Ecological anatomical study of structural-plastic response reactions of the medicinally important species *Laurus nobilis* (Lauraceae) in various ecological conditions. Plant and Fungal Research, 8(1), 23–35.
Say, A. (2024). *Peganum harmala*: A comprehensive study. In: Akgül, H., Şahna, E., & Selamoğlu, Z. (Eds.). International studies and evaluations in the field of health sciences. Amasya University, Amasya. Pp. 137–164.
Seilkhan, A. S., Kudrina, N. O., Cherepkova, N. V., & Kulmanov, T. E. (2019). Anatomical and morphological structure of *Peganum harmala* of Almaty Region and its therapeutic properties. Pakistan Journal of Botany, 51(2), 649–655.
Seven, S., & Akıncı, Ş. (2025). Effects of humic acid and salt stress on growth, physiological parameters and mineral substance uptake in *Artemisia dracunculus* L. (tarragon). Turkish Journal of Botany, 49(2), 64–79.
Shahrajabian, M. H., Sun, W., & Cheng, Q. (2021). Improving health benefits with considering traditional and modern health benefits of *Peganum harmala*. Clinical Phytoscience, 7, 18.
Singh, A., Prasad, S., & Rathore, D. (2022). Monitoring of airborne heavy metal using plants: Perspective and challenges. In: Tiwari, S., & Agrawal, S. B. (Eds.). New paradigms in environmental biomonitoring using plants. Banaras Hindu University, Varanasi. Pp. 27–44.
Tütüncü Konyar, S., Öztürk, N., & Dane, F. (2014). Occurrence, types, and distribution of calcium oxalate crystals in leaves and stems of some species of poisonous plants. Botanical Studies, 55, 32.
Ullah, H., Elahi, N. N., & Imtiaz, M. (2024). Exploring tolerable and sensitive canola varieties for cultivation with Pb contaminated municipal wastewater by using irrigation dilution technique. Pakistan Journal of Botany, 56(5), 1767–1779.
Voznesenskaya, E. V., Koteyeva, N. K., Edwards, G. E., & Ocampo, G. (2017). Unique photosynthetic phenotypes in *Portulaca* (Portulacaceae): C_3–C_4 intermediates and NAD-ME C_4 species with pilosoid-type Kranz anatomy. Journal of Experimental Botany, 68(2), 225–239.
Yadav, V., Arif, N., Kováč, J., Singh, V. P., Tripathi, D. K., Chauhan, D. K., & Vaculík, M. (2021). Structural modifications of plant organs and tissues by metals and metalloids in the environment: A review. Plant Physiology and Biochemistry, 159, 100–112.
Yirmibeş, S., Kayıhan, C., Çiçek, N., & Ekmekçi, Y. (2024). Role of sulfur metabolism in acquiring of boron tolerance in *Arabidopsis thaliana*. Turkish Journal of Botany, 48(7), 562–581.

Zhu, Z., Zhao, S., & Wang, C. (2022). Antibacterial, antifungal, antiviral, and antiparasitic activities of *Peganum harmala* and its ingredients: A review. Molecules, 27(13), 4161.